Journal of Hydrology 508 (2014) 181–196

Contents lists available at ScienceDirect

Journal of Hydrology

journal homepage: www.elsevier.com/locate/jhydrol

Isotopic and geochemical identification of main groundwater supply sources to an alluvial aquifer, the Allier River valley (France)

N. Mohammed [a,b,c,d], H. Celle-Jeanton [a,b,c,*], F. Huneau [e,f], P. Le Coustumer [d], V. Lavastre [b,c,g], G. Bertrand [h], G. Charrier [i,j], M.L. Clauzet [k]

[a] Clermont Université, Université Blaise Pascal, Laboratoire Magmas et Volcans, BP 10448, F-63000 Clermont-Ferrand, France
[b] CNRS, UMR 6524, LMV, 63038 Clermont-Ferrand, France
[c] IRD, R 163, LMV, 63038 Clermont-Ferrand, France
[d] Université de Bordeaux, EA 4592 Géoressources & Environnement, ENSEGID, 1 allée F. Daguin, F-33607 Pessac, France
[e] Université de Corse Pascal Paoli, Faculté des Sciences et Techniques, Laboratoire d'Hydrogéologie, Campus Grimaldi, BP 52, 20250 Corte, France
[f] CNRS, UMR 6134, SPE, 20250 Corte, France
[g] Université de Lyon, Université Jean Monnet, 23 rue du Dr. Michelon, 42023 Saint Etienne, France
[h] University of Sao Paulo, Instituto de Geosciências, Centro de Pesquisas de Água Subterrânea, Rua do lago, 562 Cidade universitaria, 05508-80 Sao Paulo, Brazil
[i] Clermont Université, Université Blaise Pascal, Laboratoire de Géographie Physique et environnementale, BP 10448, F-63000 Clermont-Ferrand, France
[j] CNRS, UMR 6042, GEOLAB, 63000 Clermont-Ferrand, France
[k] Clermont-Ferrand Municipality, Water Department, 10 rue Louis Rosier, 63000 Clermont-Ferrand, France

ARTICLE INFO

Article history:
Received 15 July 2013
Received in revised form 18 October 2013
Accepted 29 October 2013
Available online 6 November 2013
This manuscript was handled by Laurent Charlet, Editor-in-Chief, with the assistance of Christophe Tournassat, Associate Editor

Keywords:
Hydrochemistry
Stable isotopes
Allier River
Alluvial aquifer
Groundwater

SUMMARY

Hydrodynamic, hydrochemical, and isotopic investigations were carried out on 18 points, including boreholes, piezometers, and surface waters, from February 2011 to August 2012, to assess groundwater quality in the unconfined shallow alluvial aquifer of the Allier River (one of the main tributary of the Loire River). The study area, located near the city of Clermont-Ferrand (France), plays an important socio-economic role as the alluvial aquifer is the major source of drinking water for about 100,000 inhabitants. The objective of the project aims at understanding the functioning of alluvial aquifers that occupy a pre-eminent position in the hydrogeologic landscape both for their economic role – production of drinking water and agricultural development – and for their ecological role. Moreover, this study also targets at determining the factors and processes controlling shallow groundwater quality and origin. The water circulates from the south, with a natural alimentation from the hills in the non-pumped part of the alluvial aquifer. In the pumping zone, this general behaviour is altered by the pumping that makes the water from the Allier River enter the system in a large proportion. Four end-members have been identified for the recharge of the alluvial groundwater: rainfall, Allier River, surrounding hills' aquifer and the southern non-pumped part of the alluvial system. Results indicate that, despite the global Ca–HCO_3 water type of the groundwater, spatial variations of physico-chemical parameters do exist in the study area. Ionic concentrations increase from the Allier River towards east due either to the increase in the residence time or a mixing with groundwater coming from the aquifer's borders. Stable isotopes of the water molecule show the same results: boreholes close to the river bank are recharged by the Allier River (depleted values), while boreholes far from the river exhibit isotopic contents close to the values of hills' spring or to the southern part of the alluvial aquifer, both recharged by local precipitation. One borehole (B65) does not follow this scheme of functioning and presents values attesting of a probable sealing of the Allier River banks. Based on these results, the contribution of each end-member has been calculated and the functioning of the alluvial system determined.

1. Introduction

The Allier River (French Massif Central) is one of the main tributary of the Loire River nowadays considered as "the last wild river in the western Europe" owing to the relative absence of large dams and the consequent semi-natural condition of the river, notably in its upper reaches. For these reasons, the European Program "Plan Loire Grandeur Nature" has been settled in 1994 with the aims of ensuring the security of Loire valley's residents in case of floods, responding to the needs of water supply and protecting and restoring the river's biodiversity. This study is a part of the third phase of the Plan Loire (2007–2013) and is dedicated to the characterization

* Corresponding author. Address: Université Clermont-Ferrand 2, 5, Rue Kessler, 63000 Clermont-Ferrand, France. Tel.: +33 4 73 34 67 54.
E-mail address: celle@opgc.univ-bpclermont.fr (H. Celle-Jeanton).

0022-1694/$ - see front matter © 2013 Elsevier B.V. All rights reserved.
http://dx.doi.org/10.1016/j.jhydrol.2013.10.051

of the alluvial aquifer of the Allier River considering its fundamental ecological and socio-economical role in the Auvergne region.

In fact, due to their permeable nature, alluvial aquifers play a fundamental role by supplying large quantities of water for drinking, industrial, and agricultural purposes in many countries (Doussan et al., 1997; Guo and Wang, 2004; Chkirbene et al., 2009; Lorite-Herrera and Jimenez-Espinosa, 2008). Alluvial aquifers have a fundamental ecological significance for they sustain various aquatic and terrestrial ecosystems of high patrimonial values and an economic role bound to the presence of easily irrigable fertile zones and to the production of industrial or drinkable water in advantageous costs. Therefore, they contribute to give these systems a pre-eminent place in the socio-economical management of an area (Klove et al., 2011). In the hydrogeology of the alluvial aquifer, what is determining is not only the extension of the alluvium formations but also the relationships that these can maintain with the surroundings aquifers, the substratum and the connected surface waters. Three models of functioning of alluvial aquifers can be proposed according to their geological context: (1) either the aquifer behaves as a drain which collects and leads to the superficial water network flow stemming from neighbouring aquifers, (2) or as a very permeable environment connected to the river which recharges the aquifer with the water coming from the upstream part of the basin (3) or as a combination of both models, each playing a variable role according to the location of the investigated well with regard to both limits (Huggenberger et al., 1998). The existence of these flows of diverse origins is translated, in open limits of the alluvial systems, by waters of different chemical composition.

Groundwater chemistry of alluvial aquifers depends on natural factors such as leaching and soil–rock–water interactions (Scheytt, 1997; Stigter et al., 1998), hydrodynamical characteristics of the aquifer, quality of recharge water and interaction with surface water or neighbouring aquifers (Stallard and Edmond, 1983). Moreover, anthropogenic activities such as industrial processes, agricultural practices and the development of population (Kelly, 1997; Stigter et al., 1998; Kraft et al., 1999; Böhlke, 2002) can alter these fragile systems, either by polluting them or by modifying the hydrological cycle to such an extent that the use of groundwater becomes limited.

The study site is the main water catchment of Clermont-Ferrand, the biggest town of the Auvergne region, and provides drinking water for around 100,000 inhabitants. Land occupations with agricultural activities and population centres extend from year to year. Consequently, there is a critical need to increase the knowledge of the system from quantitative, hydrodynamic and qualitative perspectives to sustain the groundwater resource, as also required by the Water Framework Directive (European Parliament, 2000) and the Groundwater directive (European Parliament, 2006). The purpose of this study is to improve ecological and socio-economical water management not only at the site scale but also at the whole scale of the Allier watershed. In this context, hydrochemical and isotopic methods were used to identify the sources, types and quantities of various components of groundwater and to describe their spatial and temporal variations.

2. Study area sittings

2.1. General settings and geology of Allier basin

This study was performed in the Quaternary shallow alluvial aquifer of the Allier River, located in the Allier basin covering a surface of 14,310 km^2 (Fig. 1). The climate of the Allier basin is subjected to high spatial variability due to altitude variations from

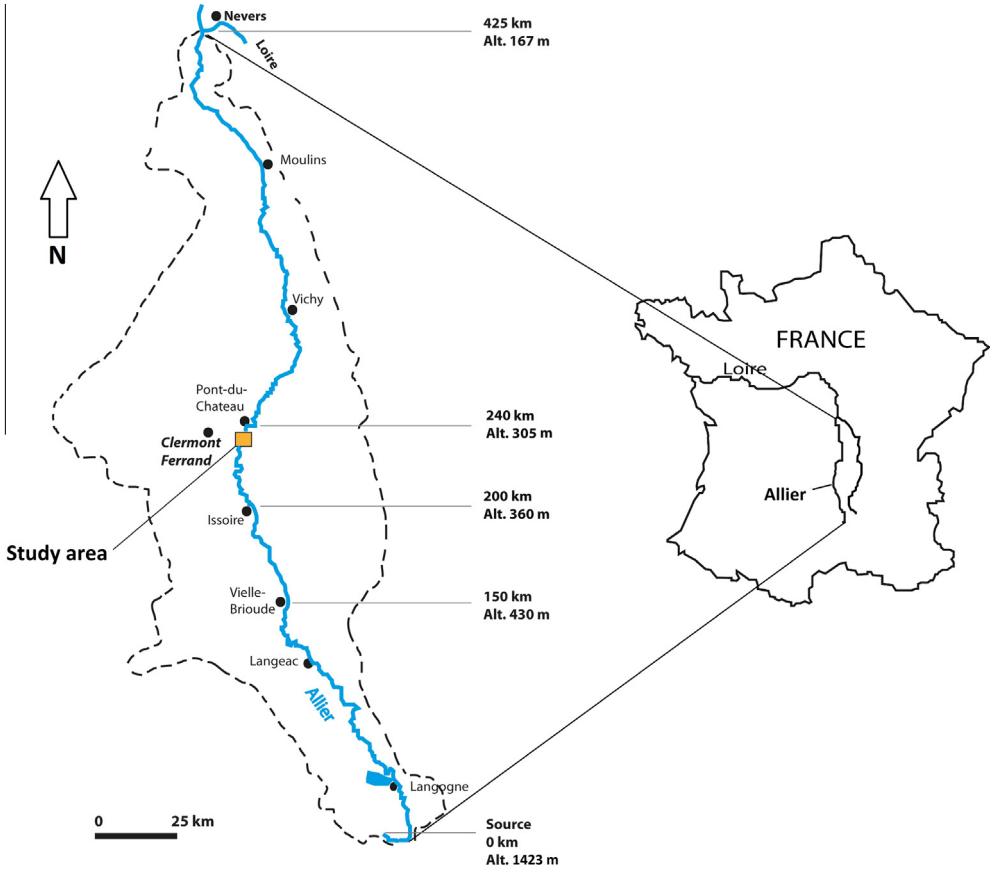

Fig. 1. The Allier River basin and the study area location.

167 to 1423 m.a.s.l. with a mean altitude of 900 m.a.s.l. and to the mixed influences of oceanic, continental climate as well as Mediterranean incomes in the southern part (Bertrand et al., 2008; Négrel and Roy, 1998). Rainfall is often different from location to another, such as in the mountainous area (upstream of study area); the maximum values are reached in winter and late spring (about 2000 mm), and the minimum ones in the summer (about 570 mm). Allier basin receives on average 800 mm of rain annually, with an average annual temperature comprised between 5 and 6 °C in the higher altitudes of the basin and 11.7 °C in the lower altitudes (Bertrand et al., 2010, 2013). The Allier River, the main tributary of the Loire River, originates in the Massif Central (La Maure de Gardille, 1423 m.a.s.l.) and flows roughly from South toward North with a total length of 410 km long; it joints the Loire River at the Bec d'Allier, near Nevers.

Geologically, the Allier River basin occupies the Limagne rift valley, an elongated tectonic depression in the Hercynian crystalline Massif Central, France (Dèzes et al., 2004). The drainage basin is underlined by Hercynian crystalline basement rocks (58%), with Cenozoic volcanic rocks (22%) mainly along the margins of the rift valley and partly calcareous Oligocene fluvio-lacustrine sediments (20%) as a rift valley fill (Korobova et al., 1997). Strong uplift of the Massif Central from the beginning of the Quaternary onwards (Dèzes et al., 2004; Ziegler and Dèzes, 2005) has forced the Allier to incise deeply into the underlying bedrock, thus forming many terraces. Furthermore, there was on-going volcanism in the uplifted rim west of the rift valley. The Allier terrace deposits are gravelly and sandy sediments poor in clay and encompassing silicate components of granitic-gneissic and basaltic origins from Massif Central, reflecting the different lithologies within the Allier basin. However, this composition is not linearly correlated with basin lithology, the volcanic components usually predominate while the Oligocene rocks are usually rare (Veldkamp and Feijtel, 1992). Common heavy minerals of the Allier terraces are augite, green and brown hornblende, olivine, mica and opaques (Van Dorsser, 1969; Rudel, 1963; Pelletier, 1971; Pastre, 1986; Tourenq, 1986). The opaque component, which can comprise more than 50% of the fine sand fraction, is predominantly composed of basaltic rock fragments. The sediment composition has known many changes in time due to incision of the Allier, glaciations of the higher parts in the basin and volcanic eruptions (Kroonenberg et al., 1988). The ancient alluvial deposits of Allier are distinguished from recent alluvial deposits. The former (Early Pleistocene) are thin, about several meters, and are consisting of quartz, sand and little clay whereas the latter alluvium is composed of sand, gravel and rocks covered with layer of silt. These alluvial deposits are mainly located over the marly calcareous deposits of the Limagne or directly on the crystalline basement (Dadet et al., 1979). The alluvial layer is 6–15 m thick (10 m on average) and their scope ranges from a few meters to several kilometres on each side of the river.

The total alluvial aquifers represent about 6% of the Allier basin, and then the total estimated volume of water contained in this alluvial layer is about 2 billion cubic meters (Livet et al., 2006). The basin's alluvial plain is used primarily for animal husbandry and agriculture (maize and cereal) which occupies about 71% of land cover of the basin, forest and grassland come next with 24% and urbanization with only 5%. The alluvial aquifer is unconfined and is in direct contact with surface water so it can be affected by surface recharge and discharge.

2.2. Settings of the sampling site

The study site is located about 20 km from the east of the city Clermont-Ferrand, France (Fig. 1). The climate of the study area is quite clement with fairly hot summer that temperatures climb to 27 °C in July and August and cold winter, temperatures of just below 0 °C in December and January. The study area has an average rainfall of 570.9 mm which is one of the lowest rates in France. Most of the rainfall falls between May and September.

Regarding to the geology (Fig. 2), the study site is in accordance with the lithology previously described with a succession of Quaternary alluvial deposits overlying Oligocene terrains consisting in marl, clay and limestone. The alluvial sediments are surrounded by hills constituted of Oligocene sediments or volcano-sediments (peperite) and Miocene volcanic formations. These terrains are characterised by high permeability and supply many springs generally located at hill foot.

Due to its importance as a fundamental source for the drinking water supply, the study area is protected and fenced. The site is active since the 1930s and accounts nowadays 71 boreholes distributed on a total surface of 2 km^2 (Fig. 3), most of them being located in the riverbanks of the Allier River. These boreholes allowed obtaining a general overview about the hydrogeological settings of the area. Water table is shallow with a depth varying from 2 to 4 m. Alluviums have a permeability ranging from 10^{-3} to 10^{-4} m/s and an efficient porosity of 8–10% (Frémion, 1995, 2007). From hydrodynamical point of view, groundwater–surface water interactions are supposed to be important along the Allier River, mainly because the river discharge and the piezometric variations are buffered in regards to the local high climate variability (Livet et al., 2006). According the water circulation/recharge and pumping, four end-members can be hypothesized: Allier River which is supposed to be the main source, surrounding hills groundwater, the southern part of the alluvial aquifer (characterised by a large non-pumping zone), and direct local recharge by effective rainfall.

3. Sampling and analytical methods

75 points (70 pumping boreholes, 3 piezometers including P13, (Fig. 3) in the no-pumping southern part of the alluvial aquifer, 1 spring emerging from the surrounding hills, and the aquifer-connected river) were sampled during two intensive field campaigns, in December 2010 (low flow conditions) and June 2012 (high flow conditions). Among these 75 points, 18 were selected for a temporal monitoring and have been sampled bi-weekly from February 2011 to August 2012 for physico-chemical and isotopic analysis. A total of 841 water samples were collected during the study period (including 684 groundwater samples from boreholes, 80 water samples from piezometers, 38 water samples from spring, and 39 Allier River water samples). In order to characterize the local recharge, 42 rainfall samples were collected weekly within the study area, during the same period, by a 614 cm^2 pluviocollector with automatic aperture (Eigenbrodt Automatic Precipitation Sampler NSA 181). By using narrow diameter submersible pump, water samples were collected in clean polyethylene bottles for major ions measurements (Ca^{2+}, Mg^{2+}, Na^+, and K^+, HCO_3^-, Cl^-, NO_3^- and SO_4^{2-}) and for silica (H_4SiO_4), and 20 mL glass bottles with poly-sealed lids for water isotopes. Sampling bottles, at the time of sampling, were thoroughly rinsed 2 times using the water to be sampled. In situ measurements including EC, pH and temperature were achieved by using a WTW Multi 3420 set C. The discharges of the springs were measured through a volumetric gauging method with a 1-L container and a chronometer. Water level of each borehole and piezometer were recorded by water-level dipper. All collected samples were transported in ice-boxes to the municipal laboratory of Clermont-Ferrand for major elements analysis.

Major cations (Ca^{2+}, Mg^{2+}, Na^+, and K^+) were analysed using mass spectrometer ICP-MS-7700, major anions (Cl^-, NO_3^- and SO_4^{2-}) were analysed using ion chromatography ICS-1000, and H_4SiO_4 was analysed by spectrophotometry. HCO_3^- was determined

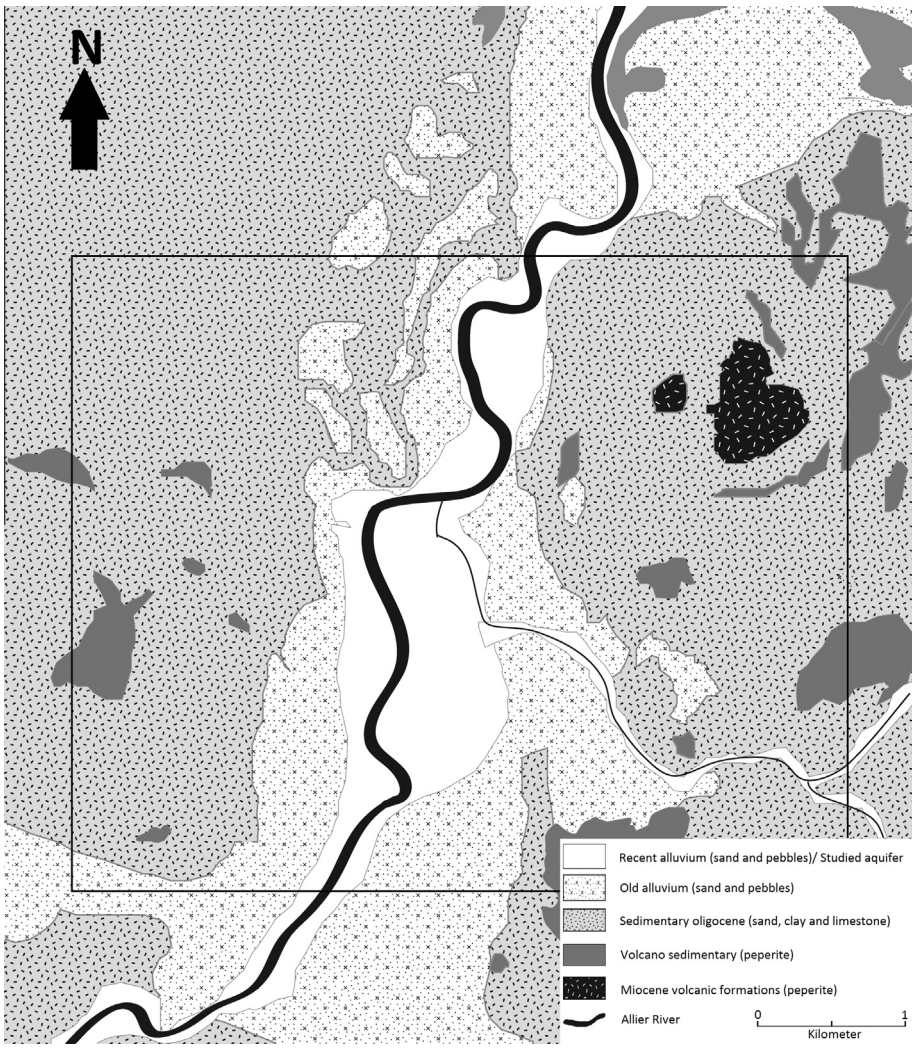

Fig. 2. Geological settings of the study site.

by titration with H_2SO_4. These analyses were run immediately after sampling. The quantification limits for was 0.1 mg/l for major cations, 1 mg/l for major anions and 0.1 mg/l for H_4SiO_4.

Isotopic analysis were performed in the Hydrogeology Department of the University of Corsica (CNRS UMR 6134 SPE), and both stable isotopes of the water molecule were characterized using a liquid-water stable isotope analyser DLT-100 (Los Gatos Research) according to the analytical scheme recommended by the IAEA (Aggarwal et al., 2009; Penna et al., 2010). The accuracy was 1‰ for δ^2H and up to 0.1‰ for $\delta^{18}O$. The isotopic data is reported in the standard delta notation in part per thousand relative to Vienna Standard Mean Ocean Water (Clark and Fritz, 1997).

4. Results and discussion

The minimum, maximum, average and standard deviation of physico-chemical, chemical and isotopic data of the 18 points used for the temporal monitoring of the system are summarized in Table 1.

4.1. End-member characteristics

Taking into account the circulations of water in alluvial system, the chemical composition of groundwater is influenced by four potential end-members: Allier River, hills located in the east side, southern non-pumped alluvial aquifer, and local precipitation. Direct recharge from Allier River is the main source of groundwater in the pumping area. The river flow rate is described through three different periods (Fig. 4a): (1) low flow rate of around 9.6 $m^3 s^{-1}$, during the two or three warmest months in the summer, (2) high flow in winter with flood impulses that can reach 377.6 $m^3 s^{-1}$, and (3) high flow in spring (176 $m^3 s^{-1}$) that corresponds to snow melting in the higher part in the basin; the average flow rate is of 40.4 $m^3 s^{-1}$. The electrical conductivity of the Allier River is generally low (mean for the sampling period = 183 μS/cm) and do not present any significant seasonal variation (Fig. 4d). However, a significant negative correlation between flow rate and electrical conductivity observed in Allier River (Fig. 4a and d). As a surface water, seasonal variation of temperature has been detected (Fig. 4c) with values that vary from 0 °C (14/2/2012) to 21.2 °C (14/8/2011). The Allier River's water type is Ca–Na–Mg/HCO_3–Cl (Fig. 5) in accordance with the leaching of the water catchment's basement mainly constituted of granitic and gneissic rocks. One exception concerns the 7/11/2011 analysis characterized by a Ca–Na–Mg/Cl–HCO_3 facies. This particular water has been during a flood event and then corresponds to major dilution effect with an electrical conductivity of 79 μS/cm; the change in water facies could be explained by the low concentration in ions.

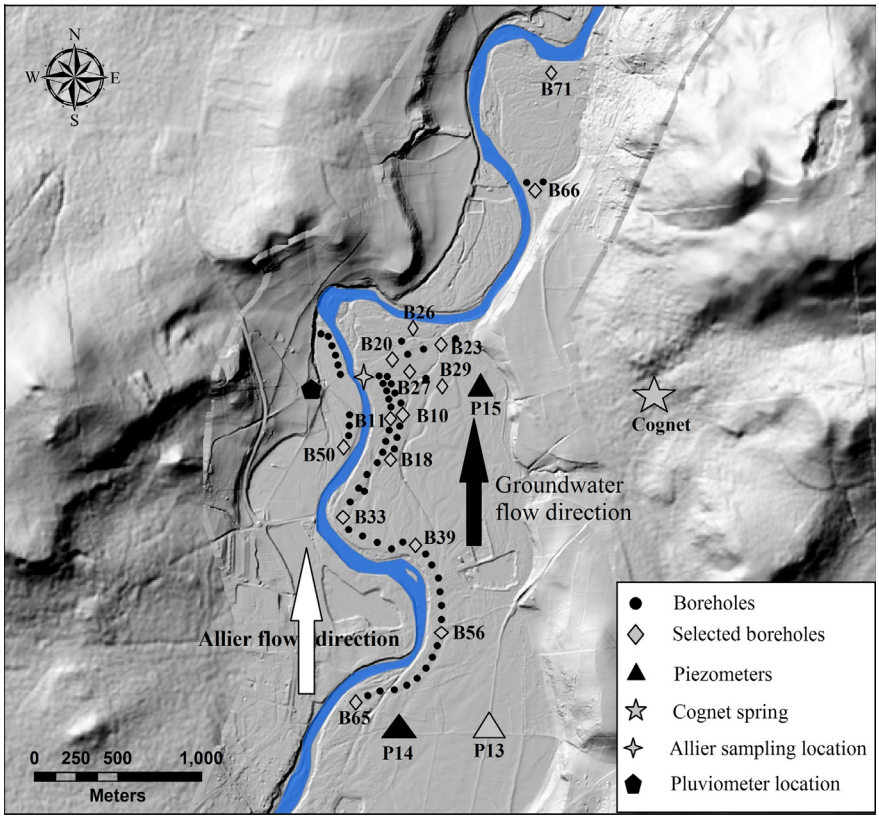

Fig. 3. Locations of sampling points.

Water coming from the hills constitutes the natural recharge origin of the alluvial groundwater. This source is represented by Cognet spring which shows a high EC varying from 818 to 1061 μS/cm (Fig. 4d). This sampled point is also characterised by high content of nitrate, sulphate and potassium with a mean concentrations of 49.6, 36.7 and 17.9 mg/l, respectively. These ions are primarily anthropogenic and mainly from agricultural sources, since the hills are extensively using for agricultural practises. The temperature varies seasonally from 9.6 to 14.8 °C but in lesser degree compare to Allier (Fig. 4c). The flow rate of Cognet demonstrates a continuous decrease in 2011 and starts to increase in the beginning of 2012 till the end of July. No correlation is observed between Cognet spring's flow rate and precipitation height, highlighting possible extractions of groundwater that, for agricultural or individual supplies within Cognet's basin up the spring (Fig. 4b). The dominating water type for Cognet is Ca–Mg/HCO_3 (Fig. 5) correlated with the circulation within Oligocene sediments.

The southern alluvial aquifer (non-pumped area) also accounts in the recharge of the alluvial system. This part is represented by piezometer P13 and has the highest EC recorded within the site, during the sampling period, that reaches 1541 μS/cm, what might likely be due to the slow circulation of groundwater in this non-pumping area (mean EC = 1194 μS/cm). Except for the measurement of 28/02/2011, the EC values are stable and do not show any seasonal variations (Fig. 4d). Furthermore, it contains very significant amounts of [NO_3^-] and [SO_4^{2-}] with mean concentrations of 38.1 mg/l and 117.5 mg/l respectively showing anthropogenic influence from agriculture. Temperature changed seasonally in this piezometer similarly to Cognet (Fig. 4c), nevertheless, no seasonal evolution is detected in piezometric level that remains unchanged during the study period, since it is located in the no-pumping zone (Fig. 4b). This point is featured by Ca–Mg/HCO_3 water types (Fig. 5).

Lastly, local precipitation is a natural source of recharge but contains very low amounts of ions. Minimum and maximum values of each chemical parameter of rainfall (Table 1) highlight the high variability of the chemical composition and mineralization of rainwater. Bertrand et al. (2008) and Négrel and Roy (1998) found similar values at Opme station (15 km to the West from our study location) and Sainte-Marguerite (9 km to the South from our site), respectively, and argue that this variability can either be due to the rain amount (Hicks and Shannon, 1979) or to diversity in the origins of air masses (Celle-Jeanton et al., 2009). Concentrations supplied by rainfall to groundwater can be calculated by using the following equation (Appelo and Postma, 1993):

$$\text{Concentration factor} = (P/Peff) * WM_{ion} \quad (1)$$

where P is the total volume of annual precipitation, Peff refers to the efficient rainfall (Peff = the total volume of annual precipitation – total annual evapotranspiration) and WM is the volume-weighted mean of each ionic concentration for the period of measurements. The calculations give the major ion concentrations of the local recharge by rainfall (HCO_3^- = 17.8 mg/l, Cl^- = 4.8 mg/l, NO_3^- = 3.5 mg/l, SO_4^{2-} = 1.1 mg/l, Ca^+ = 1.2 mg/l, Mg^{2+} = 0.1 mg/l, Na^+ = 0.4 mg/l, K^+ = 0.1 mg/l, values are volume-weighted means).

4.2. Geochemical characteristics of alluvial groundwater

Groundwater from the 71 boreholes sampled during the study present a Ca/HCO_3 facies due to both lithology and the dissolution ability of the minerals' ions; this type is recognize in many alluvial systems around the world (in Europe: e.g. Andrade and Stigter, 2011, in Asia: e.g. Chkirbene et al., 2009). Based on secondary cations, this water type evolves from Ca–Na–Mg/HCO_3–Cl, Ca–Mg–Na/HCO_3–Cl recorded in the closest boreholes from the riverbanks to Ca–Mg/HCO_3 for the boreholes located in the eastern part of the

Table 1
Physico-chemical measurements, major ions concentrations (mg/l), oxygen-18 and deuterium data (‰ VSMOW).

Sample ID		T (°C)	pH	EC (μS/cm)	H_2SiO_4	HCO_3	Cl	NO_3	SO_4	Ca	Mg	Na	K	δ^2H (‰)	$\delta^{18}O$ (‰)
Rainfall	Min		5.6	3.1		2	<1	<1	<1	<1	<1	<1	<1	−133.6	−17.5
	Max		8.5	32		43	4	7.5	2.4	3.1	0.3	1.7	0.8	−8.2	−1.9
	Av		7.1	14.1		7.6	0.4	1.6	0.5	0.6	0.1	0.3	0.1	−47.2	−6.3
	V-WM		6.6	11.1		7.0	0.09	1.3	0.4	0.5	0.03	0.13	0.04	−46.3	−6.4
	SD		0.6	7.5		8.7	0.9	1.6	0.7	0.7	0.1	0.4	0.2	26.1	3.4
Allier	Min	2.5	7.1	79	6.2	24	6.7	2.5	4.5	6.2	2.2	5.6	1.7	−65.7	−9.4
	Max	21.2	7.9	350	16.3	98	20.8	6.9	10.4	20.3	6.8	17.9	6.2	−49.5	−7.0
	Av	13.4	7.5	183	11.6	68.9	15.2	4.6	8.1	14.3	5	12.5	3.4	−55.4	−8.1
	SD	5.9	0.2	48.2	2.6	16	3.8	1	1.4	3.2	0.9	3	0.8	3.4	0.6
	Min	9.6	6.9	818	19.9	421	29.6	38.3	31.7	102.8	32.3	14.1	14.5	−51.0	−7.5
Cognet	Max	14.8	7.7	1061	47.7	521	50.2	55	41.9	148.4	41.8	19.6	22.9	−49.0	−6.7
	Av	12.9	7.3	951.3	38.8	484.5	35.3	49.6	36.7	123.5	38.1	15.8	17.9	−50.3	−7.0
	SD	1.2	0.2	53.1	5.3	23.2	5.4	4.1	2.3	9.9	1.8	1	1.6	0.5	0.2
	Min	9.1	6.6	1099	21	489	57.2	29.4	91.8	129.3	48.9	28.6	9.3	−48.8	−6.8
P13	Max	14.7	7.3	1541	42.4	554	109	51.2	143.8	168.9	58.5	44.1	14.3	−44.6	−5.8
	Av	12.2	7.1	1192	31.1	513.7	68.4	38.2	117.5	142.4	52.5	34.1	10.9	−46.6	−6.2
	SD	1.4	0.1	77.2	3.8	13.1	9.2	5.8	12.8	8.2	2.3	3.8	1.2	1.0	0.3
	Min	9	6.8	221	7.7	90	15.7	4.3	10.1	21.7	7.2	11.9	2.6	−56.4	−8.6
B10	Max	14.6	7.3	509	22.6	203	29.5	20.7	46.3	56	18	20.1	6	−51.1	−7.1
	Av	12.4	7.1	358.2	19.3	147.6	21.1	10.5	24.1	35.5	12	16	4.3	−54.1	−7.9
	SD	1.4	0.1	85.6	2.6	31.1	4.4	5.8	11	10	3.3	2.1	0.9	1.4	0.4
	Min	8.5	6.8	152	4.4	59	10.4	2	6.4	11.4	3.9	8.9	2.1	−59.4	−8.9
B11	Max	16.7	7.5	271	21.2	96	20.3	7.3	9.7	20.7	6.1	15.4	5	−50.0	−7.1
	Av	12	7.1	195.3	14.6	75.9	14.5	4.4	8	15.9	5.1	11.6	3	−55.6	−8.2
	SD	2.2	0.1	25.9	2.7	11.5	2.7	1.4	0.8	2.7	0.6	1.5	0.7	2.7	0.5
	Min	9.6	6.9	203	7.2	87	13.3	<1	6.5	18.9	5.2	9.8	2.3	−58.1	−8.7
B18	Max	15.9	7.3	244	22	116	16.7	3.2	8.1	25.8	6.5	13.9	3.7	−54.1	−7.8
	Av	12.7	7.1	221.9	17.9	99.7	14.8	1.1	7.2	21.2	5.9	12.1	2.9	−56.0	−8.3
	SD	1.3	0.1	7.7	3.2	4.9	1	0.7	0.4	1.6	0.3	0.8	0.4	1.0	0.2
	Min	9.5	6.9	188	7.7	76	11.3	1.6	7.2	15.3	4.6	8.9	2.3	−59.1	−8.8
B20	Max	14.5	7.3	251	20	107	19.4	5.3	9.9	22.5	7.1	14.4	4.2	−50.8	−7.3
	Av	12.2	7.1	210.4	16.5	87	15	3.7	8.7	18.8	5.7	11.9	3.1	−55.8	−8.2
	SD	1.2	0.1	18.4	2.3	8.8	2.3	1.2	0.6	2	0.6	1.2	0.5	2.3	0.4
	Min	9.8	6.8	384	6.8	189	18.5	7.5	22.7	36.2	15.6	15	6.1	−52.4	−7.8
B23	Max	15.1	7.5	1001	37.5	526	42	26.2	91.4	130.7	51.2	31.4	13.6	−45.1	−5.2
	Av	12.6	7.3	830.3	21.7	400.6	33	18.9	62.4	90	37	24.6	10	−49.6	−7.0
	SD	1.4	0.1	162.9	5.8	103.1	6.1	4.3	16.1	24.9	9.7	3.4	1.6	2.0	0.5
	Min	6.6	6.9	154	4.2	63	9.8	<1	6.1	12.5	3.8	9	1.1	−60.5	−9.0
B26	Max	19.5	7.7	250	20.5	104	21.2	7.2	11.5	25.5	7.2	16.3	4.7	−50.0	−7.0
	Av	12.3	7.3	205.2	14.3	83.4	15.2	4.2	8.5	18.5	5.3	12	2.9	−55.8	−8.2
	SD	4.4	0.2	25.4	3.1	11.6	3.4	1.8	1.2	3	0.7	1.9	0.8	3.0	0.5
	Min	9.3	7	265	9	117	14.4	5.4	12	25.4	8.5	13.3	2.9	−55.5	−8.3
B27	Max	14.6	7.3	682	21.8	292	38.3	19.6	58.1	75.2	26.5	28.6	7.7	−47.5	−6.3
	Av	12.7	7.2	459	18.3	197.6	25.1	12.5	34.9	47.7	16.5	19.1	4.7	−51.5	−7.4
	SD	1.3	0.1	119.6	2.9	48.1	6.8	5.5	14.8	14.9	5	3.5	1.1	2.1	0.5
	Min	9.2	6.9	912	10.1	451	42.5	12.8	69	76.2	44.9	30.2	9.4	−47.1	−6.3
B29	Max	15.6	7.5	1005	35.8	503	54.5	26.2	83.7	117.3	64.3	58.1	18.5	−42.5	−5.6
	Av	13.1	7.3	972.8	22.7	474	48.7	21.1	76.3	96.8	49.9	37.8	11.5	−45.2	−6.0
	SD	1.5	0.1	19.2	4.3	11.8	2.3	2.6	3.7	6.2	3.3	4.5	1.6	1.1	0.2
	Min	6.2	6.8	155	5.4	61	9.2	1.6	6.4	11.5	4.1	10.1	2	−58.7	−8.9
B33	Max	19.4	7.6	242	24.7	90	21.2	6.8	11	19	6.3	17.5	5.2	−50.1	−7.0
	Av	12.4	7.1	193.1	14.5	74.2	14.8	4.7	8.2	15.3	5.2	12.4	3.2	−55.3	−8.1
	SD	4.3	0.2	24.6	2.8	9.2	3.5	1.4	1.1	2	0.5	2	0.8	2.6	0.5
	Min	9.8	6.9	181	6.3	73	10.7	<1	4.9	13.9	4.5	8.9	2.2	−59.0	−8.8
B39	Max	16	7.8	252	21.9	116	19.9	3.7	7.9	25	7.2	14.9	4.8	−49.7	−7.2
	Av	12	7.3	205.1	17.2	89.4	14.5	0.9	6.4	17.2	5.8	11.8	3.3	−55.4	−8.3
	SD	1.9	0.2	21.8	3.2	11.4	2.4	0.7	0.8	2.5	0.7	1.5	0.6	2.8	0.5
	Min	8.1	6.8	179	6.6	72	10	3.7	7.8	17.3	4.9	8.8	2.5	−59.8	−8.9
B50	Max	18.3	7.4	808	22.2	345	43.1	35.4	62	68.9	35.7	38.1	16.3	−50.1	−6.9
	Av	13.1	7.2	377.3	16.4	158.5	22.7	12.8	23.1	37.3	11.9	18.1	5.5	−54.5	−8.0
	SD	3	0.1	142.6	2.8	63.4	8.5	6.8	12.4	14.4	6.3	5.9	2.8	2.5	0.5
	Min	7.4	6.7	159	9.5	68	9.4	1.5	7.1	14	4.7	9.2	2.5	−58.7	−8.7
B56	Max	15.1	7.6	552	21.9	233	30.2	21	36.9	57	22.3	18.7	6.9	−48.7	−7.2
	Av	11.4	7.1	310.5	17.8	131.4	18.5	7.3	17.3	29.9	10.8	13.3	4.3	−53.8	−7.9
	SD	1.9	0.2	98	2.6	42.6	5.2	4.8	8.9	11.3	4.4	2.4	1	2.0	0.4
	Min	10.4	6.8	338	8.8	161	15.8	<1	19.7	33.7	12.8	15	3.5	−44.1	−5.9
B65	Max	14.6	7.4	467	24.5	227	24.4	10.1	31.2	53.4	18.5	21.6	7	−29.3	−2.4

Table 1 (*continued*)

Sample ID		T (°C)	pH	EC (µS/cm)	H_2SiO_4	HCO_3	Cl	NO_3	SO_4	Ca	Mg	Na	K	δ^2H (‰)	$\delta^{18}O$ (‰)
	Av	12.8	7.1	425.7	19.8	200.2	21.5	1.9	26.5	42.2	15.1	19	5	−35.3	−3.9
	SD	1.1	0.1	31.4	3.5	17.2	2	2	2.6	4.2	1.2	1.5	0.8	4.2	1.0
	Min	8.8	6.9	224	5.1	98	11.9	<1	5.4	20.2	6.2	10.6	2.2	−57.6	−8.6
B66	Max	19.3	7.5	351	21	154	22.6	9.2	17.2	33.5	12.9	25.3	6.4	−49.9	−7.1
	Av	13.1	7.2	260.9	16.4	116.4	16.4	3.7	10.4	24.9	8.1	13.8	3.5	−54.6	−8.0
	SD	3.1	0.1	35	2.6	15.7	2.6	2.9	3	3.7	1.9	2.5	0.9	2.2	0.4
	Min	8.4	6.9	240	6.7	106	14.9	<1	8.7	22.8	7	10.1	2	−57.0	−8.4
B71	Max	14.3	7.5	422	24.8	185	26.6	14.6	37.5	46.1	17.8	17.3	6.4	−49.8	−7.0
	Av	12	7.2	289.6	19.6	128	17.3	4.7	13.4	29	8.9	13.8	3.2	−54.5	−8.0
	SD	1.6	0.1	57.1	3	23.6	2.8	3.4	7.2	6.6	3	1.6	1	1.8	0.4

T: temperature, EC: electrical conductivity, Min: minimum, Max: maximum, Av: arithmetic average, SD: standard deviation, V-WM: volume-weighted mean for precipitation.

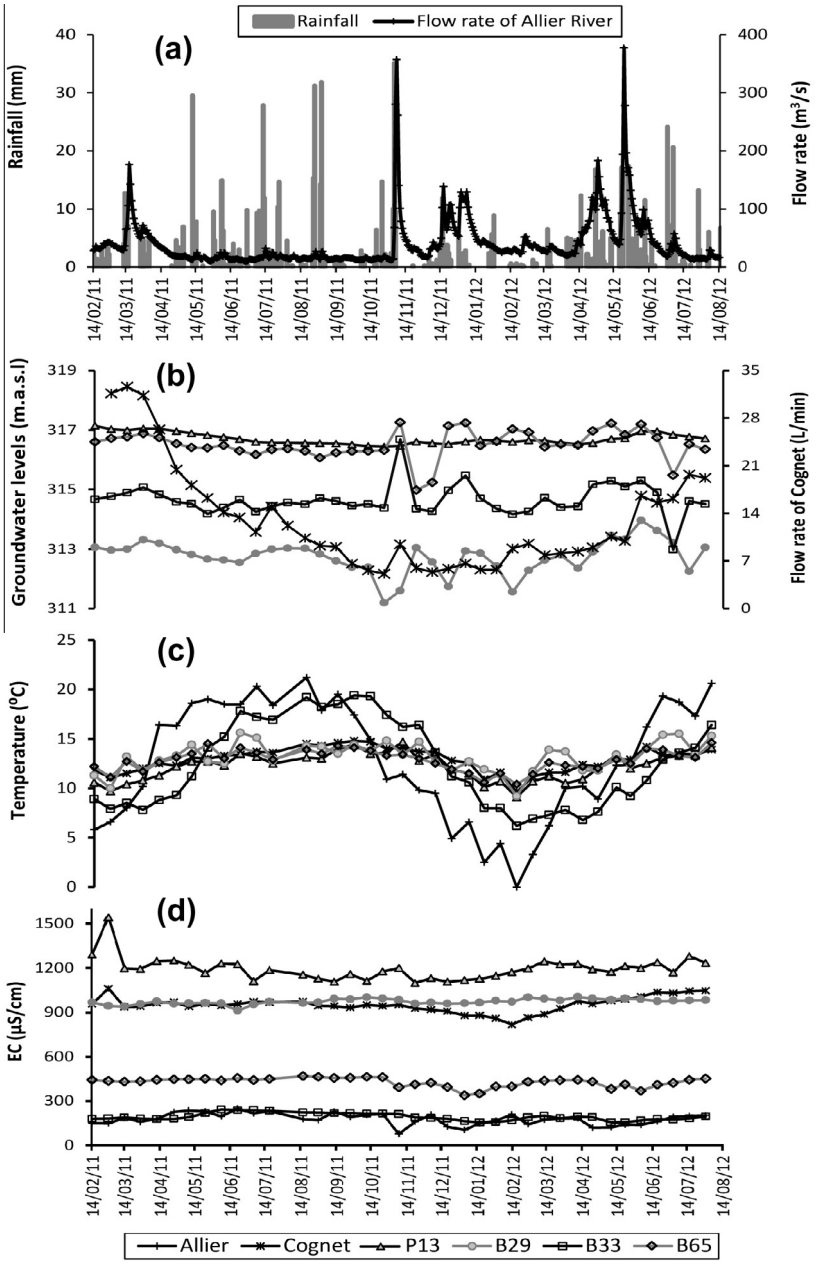

Fig. 4. Relation of (a) precipitation and Allier River flow, (b) groundwater level and Cognet spring flow, (c) temperature, and (d) electrical conductivity of selected points during study period.

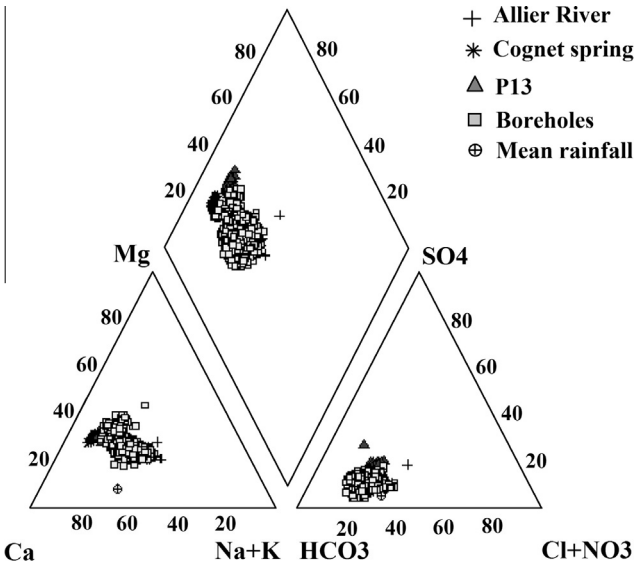

Fig. 5. Piper diagrams illustrating the chemical water types of the 18 points selected for the temporal following.

site (Fig. 5). The pH varies from 6.69 to 7.78, these values fall within natural water pH usually ranging between 6.5 and 9.5. Electrical conductivity (EC) values measured during the 2 intensive campaigns, carried out in December 2010 (low flow conditions) and June 2012 (high flow conditions), show a great spatial variation in boreholes and vary from 151 to 1005 µS/cm from the Allier River's banks to the hills' foot; values acquired in spring are lower due to the high flow period (Fig. 6). These punctual observations are completed by the following time sampling: mean ECs of the 15 boreholes sampled every 15 days show the same evolution (Fig. 7).

Variations in temperature and water level of the 15 boreholes confirm this eastward evolution. Fig. 4a–d presents the water level, temperature and EC evolutions for the four end-members and a selection of 3 boreholes: B33 close to Allier River, B29 close to hills' foot and B65, the most southern borehole. The temperature recorded in B33 shows a clear seasonal evolution, a little bit attenuated (temperature ranges between 6.2 and 19.4 °C) and with a small delay compare to Allier River. These modifications, compared to the evolution of Allier River parameters, are greater for B29 where temperature varies only from 9.2 to 15.6 °C. B29, B65, P13 and Cognet spring present the same evolution of temperature, highlighting an attenuation of air temperature variation. The same observation can be made for water level. B33 presents an evolution that corresponds to the one of the Allier River flow rate. B29 presents some high peaks that can be correlated to the increase in the River flow rate; however, the beginning of the curve shows a clear high water level that may be due to another factor. Concerning the electrical conductivity, values of B33 are in the same range of order than Allier and are low compare to the other points. The highest EC is the one of P13 (mean of 1192 µS/cm), for this point is located in a no-pumped zone. Allier flow rates show direct influence on the ionic concentrations of some boreholes, such as B10, B11, B23, P26, P33, B50, B56, B65, and B66, while the rest of boreholes show not affected. This correlation is shown in Fig. 4a and d for some boreholes.

These first observations, increase in EC and modifications of groundwater facies, highlight a general spatial evolution of groundwater chemistry from the Allier River to the eastern part of the study area. This could be due either by an increase in the residence time within the aquifer that results in higher EC and modification of water type, thanks to the dissolution of in-situ minerals, or a mixing with water from another origin, more concentrated and characterised by a different geochemical water type.

4.3. Stable isotope (δ^2H and $\delta^{18}O$) composition of water

In order to confirm these first hypotheses on the sources of recharge, stable isotopes of the water molecule have been used (Fontes, 1980; Gonfiantini, 1986; Nativ and Riggio, 1989; Wood and Sanford, 1995; Clark and Fritz, 1997). The relationships between δ^2H (‰ vs. SMOW) and $\delta^{18}O$ (‰ vs. SMOW) are shown in Fig. 8 for water collected from 18 sampling points. The 42 rain samples collected weekly define the local meteoric water line (LMWL: $\delta^2H = (7.7 \pm 0.2)\ \delta^{18}O + (1.7 \pm 1.1)$); the volume-weighted mean of

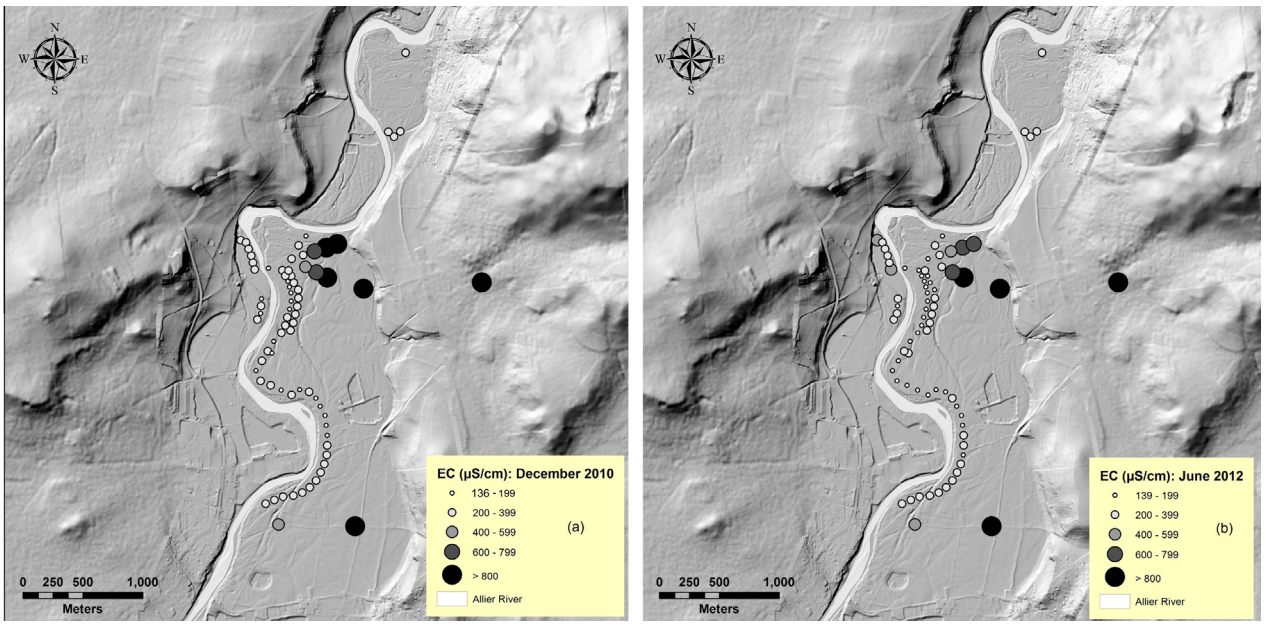

Fig. 6. Spatial distribution of electrical conductivity of 75 points during the two intensive campaigns, (a) December 2010 (low flow period) and (b) June 2012 (high flow period).

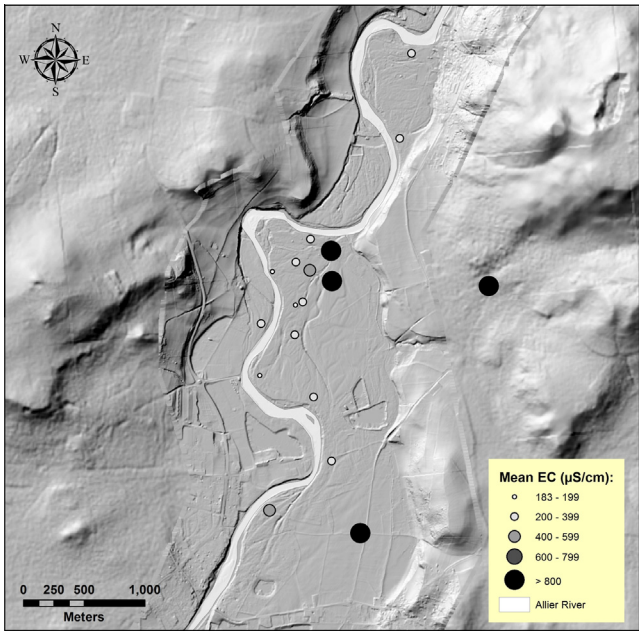

Fig. 7. Spatial distribution of the mean electrical conductivity of the 18 points selected for the temporal following. The mean value is calculated for the February-2011 to August-2012 period.

$\delta^{18}O$ and $\delta^{2}H$ for local precipitation are −6.4‰ and −46.3‰, respectively. The LMWL of the study site can be compared to the meteoric water line found in the region by by Bertrand ($\delta^{2}H = 7.9\ \delta^{18}O + 7.3$, 2009) for the Argnat Basin localized in the Chaîne des Puys (elevation = 550 m) and Gal ($\delta^{2}H = 7.8\ \delta^{18}O + 5.5$, 2005) in Saint-Just-Saint-Rambert (elevation = 420 m). Slopes are quite similar and correspond to the WMWL; difference of y-intercepts may be due to an increase of evaporation within the air column below the air masses considering that our sampling site is situated at a lower elevation. The developed LMWL is controlled by local climatic factors i.e. the origin of vapour mass, re-evaporation during rainfall and the seasonality of precipitation (Clark and Fritz, 1997) and then differs from the Global Meteoric Water Line (GMWL; $\delta^{2}H = 8\ \delta^{18}O + 10$) defined by Craig (1961). Such a difference mainly lies with a secondary evaporation during rainfall (Friedman et al., 1962) as the study site is characterised by very warm summer and generally low intensity rain events. Consistently, only 38% of the total rainfall amounts participate to the recharge (Bertrand et al., 2008).

In the 15 selected boreholes, $\delta^{18}O$ varies from −9.0‰ to −2.4‰ with an average value of −7.5‰ ($n = 560$); $\delta^{2}H$ varies between −60.5‰ and −29.3‰ with an average value of −52.4‰. The mean isotopic content of the Allier River (−8.1 $\delta^{18}O$‰ and −55.5 $\delta^{2}H$‰) which represents the input signal on the whole upstream watershed (altitude from 305 to 1423 m.a.s.l.), falls on the GMWL, in agreement with Négrel et al. (2003). P13 and Cognet spring present values close to the LMWL, testifying of a recharge of local precipitation. The isotopic signatures of most boreholes fall on, or close to the GMWL and behave similarly to Allier, demonstrating a strong interaction with the Allier River. Few boreholes (B23, B27, and B29) present more enriched values, close to the values of Cognet and P13 and drop into LMWL, indicating that these points could partly or highly be recharged by other sources than Allier River. Likewise, waters from boreholes are distributed along a line with a smaller slope than the LMWL that may indicate either evaporation or mixing trend between the two poles defined by Allier River and local recharge. This last hypothesis is consistent with the fact that the isotopic content of groundwater varies along with the distance from the two end members. In contrast to this general trend, borehole B65, harbouring the most enriched $\delta^{18}O$ and $\delta^{2}H$, (ranging from −5.9‰ to −2.4‰ and from −44.1‰ to −29.3‰, respectively), shows evidence of some additional isotopic enrichment by either stronger evaporative process or mixing with geothermal water. Indeed, the Allier basin is characterized by the availability of localized geothermal springs (Rihs et al., 2000; Bertrand et al., 2013). Measurements in carbon-13 of total dissolved inorganic carbon show that this geothermal effect cannot be implied as the values of B65 are comprised between −16.3 $\delta^{13}C$‰ and −10.3 $\delta^{13}C$‰ PDB far from the local signature of mantellic CO_2 degassed in the Chaîne des Puys (−6.6 ± 0.8 $\delta^{13}C$‰) determined by Batard et al. (1982).

From the temporal monitoring of selected points in the plain, a clear simultaneous seasonal evolution on $\delta^{18}O$ can be quoted for Allier River and B33 with a little delay in B33 peaks, highlighting this borehole is mainly supplied by the Allier River (Fig. 9). B29, Cognet spring and P13 present enriched and more stable values, demonstrating the absence of a rapid supply to the system for these points. The particular B65 point seems to be disconnected from the variations of rainfall height, but is however related to the fluctuations of the Allier River flow rate. Recorded isotopic values of B65 decrease during high flow periods and increase during low flow; this could imply a sealing of a part of the banks of the riv-

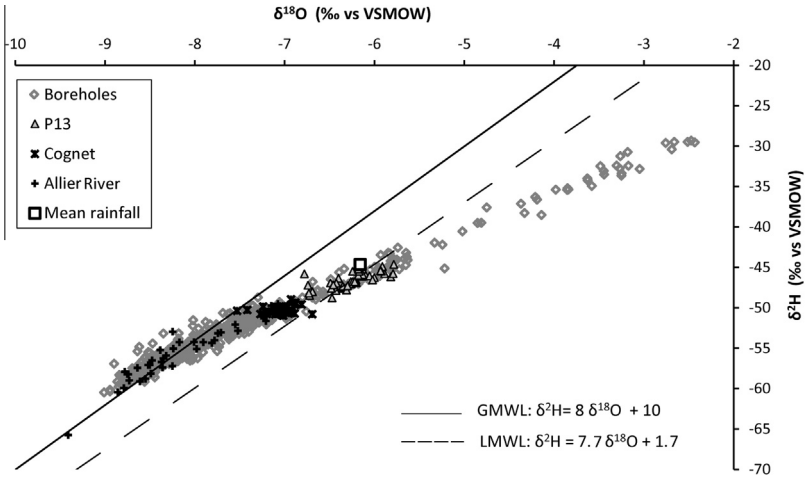

Fig. 8. $\delta^{18}O$ versus $\delta^{2}H$ (‰ vs. SMOW) in the 18 points selected for the temporal following.

er near B65. The water infiltrated from the Allier River or coming from the southern part of the aquifer evaporates during the low flow periods and is mixed with new water coming from a reconnection of the Allier River during the high flow periods. The spatial and temporal distribution of stable isotopes of $\delta^{18}O$ and $\delta^{2}H$ of the 75 sampling points during the two campaigns are shown in the Fig. 10.

The results of isotopes confirm the hypothesis formulated thanks to physico-chemical parameters, with a possible increase of the residence time of water that may lead to evaporation in such shallow aquifers (Mook, 2000) and consequently to an isotopic enrichment. A secondary supply with water isotopically enriched could also explain this hypothesis. In order to precise the geochemical processes involved along with the groundwater flow-path, the spatio-temporal evolution of mineral dissolution is discussed in the following.

4.4. Water–rock interactions

The plot of Na/Ca vs HCO_3^- for the 15 selected boreholes reflects the geology of the water basin (Fig. 11a). The Allier River that totalises the influences of the whole watershed clearly presents enrichment in $[Na^+]$ in relation with the crystalline nature of the basement. The boreholes samples present a progressive enrichment in $[Ca^{2+}]$ and $[HCO_3^-]$ between Allier River end-member and a pole represented by Cognet spring/P13. This evolution is confirmed by Fig. 11b plotting Ca + Mg vs HCO_3^-. A progressive enrichment in $[Ca^{2+}]$, $[Mg^{2+}]$ and $[HCO_3^-]$ is registered from the Allier River to the hills/southern aquifer that suggests an increase in the residence time within the aquifer and might reflect carbonate dissolution as the presence of significant proportion of carbonates in the basin has already been reported (Négrel et al., 2004). A mixing with water that circulates in carbonates is also possible as the abundance of Ca^{2+}, Mg^{2+} and Na^+ ions can be associated with minerals available in the alluvial terraces in the study area such as augite, green and brown hornblende, olivine, mica and opaque (Pelletier, 1971; Pastre, 1986; Tourenq, 1986). The presence of H_4SiO_4 in Cognet spring, boreholes, P13 and surface water suggests that crystalline rock fragments form a major component of aquifer matrix. H_4SiO_4 is present in all water samples at high concentrations but Cognet spring had the maximum concentration with a mean value of 38.8 mg/l, higher than the mean value of 17.7 mg/l in boreholes.

Thus, weathering and erosion of rocks or soil, and chemical reactions beneath the land surface control the natural composition of groundwater (Bullen et al., 1996; Kim, 2002). In this study, saturation indices (SI) of carbonate minerals (calcite and dolomite), and siliceous minerals (quartz and chalcedony) were calculated by using PHREEQC program (Parkhurst and Appelo, 2003). The summary statistics of saturation indices of some common mineral phases is presented in Table 2 and Fig. 12. All the samples are saturated with respect to quartz and/or chalcedony confirming the crystalline nature of the basin basement. Boreholes close to Allier River (e.g. B33) are undersaturated with respect to carbonate minerals indicating either that the groundwater originates from an environment where carbonate minerals are poorly available or/and due possibly to the short residence time of groundwater within this borehole, so that there is inadequate time for mineral phases to react to reach equilibrium. While, water samples from Cognet spring, P13 as well as both boreholes B23 and B29 are shown over saturated with respect to carbonate and siliceous minerals, suggesting that waters involved in their chemical composition have possibly longer residence time and consequently have dissolved more minerals.

The results show a progressive increase in the SI with respect to chalcedony and quartz from the Allier River to Cognet (B33–B10–B29) in relation with the dissolution of alluviums of crystalline origin (siliceous pebbles, sands, silts) and the volcano-sedimentary nature of the hills. This could suggest that the increase in the residence time is a major process in the chemical composition of waters. Regarding the evolution of SI with respect to dolomite and calcite, B33 and B10 are clearly undersaturated and show

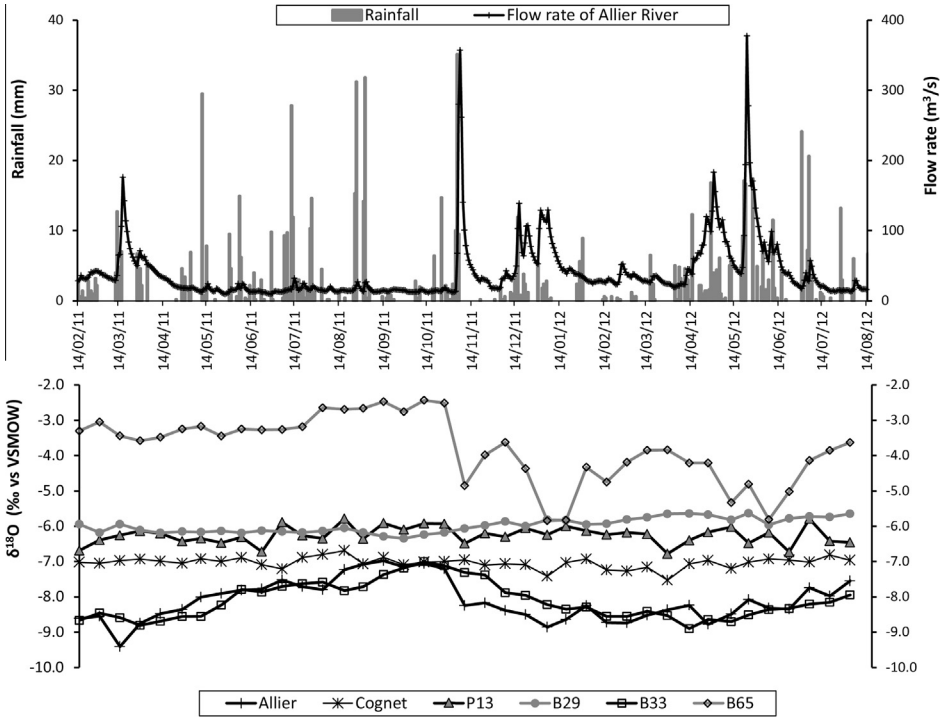

Fig. 9. Temporal variations in Allier flow rate and $\delta^{18}O$ of three boreholes (B33, B65, B29), Allier River, Cognet spring and piezometer P13.

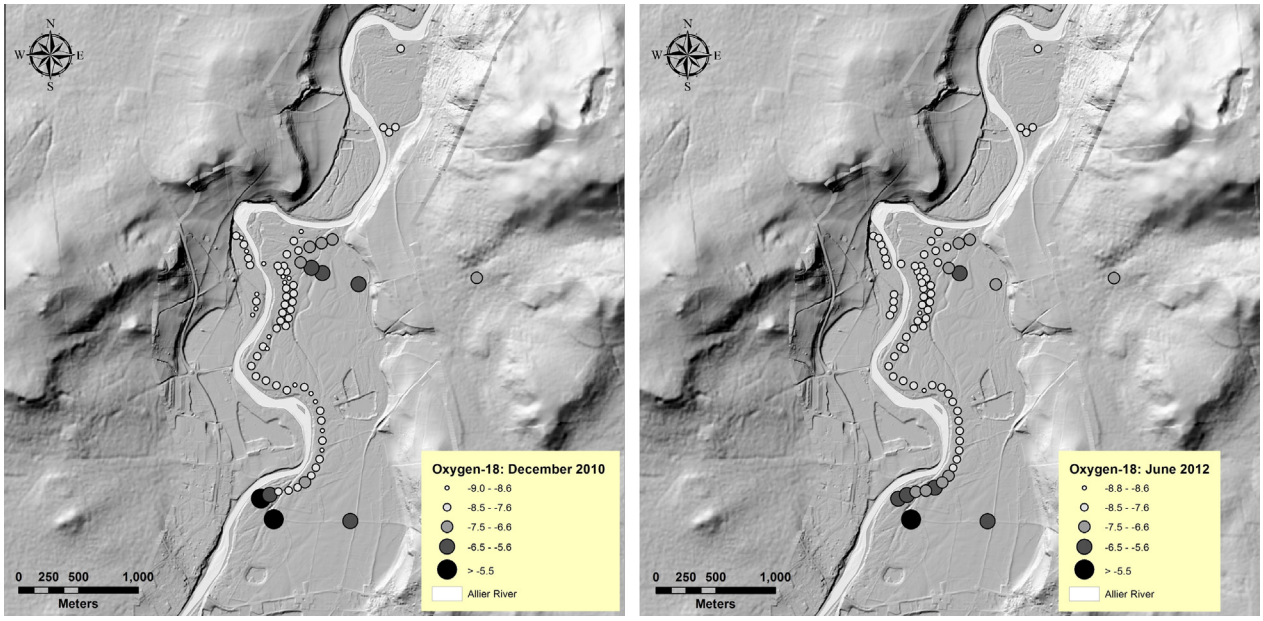

Fig. 10. Spatial distribution of $\delta^{18}O$ of 75 points during the two intensive campaigns, (a) December 2010 (low flow period) and (b) June 2012 (high flow period).

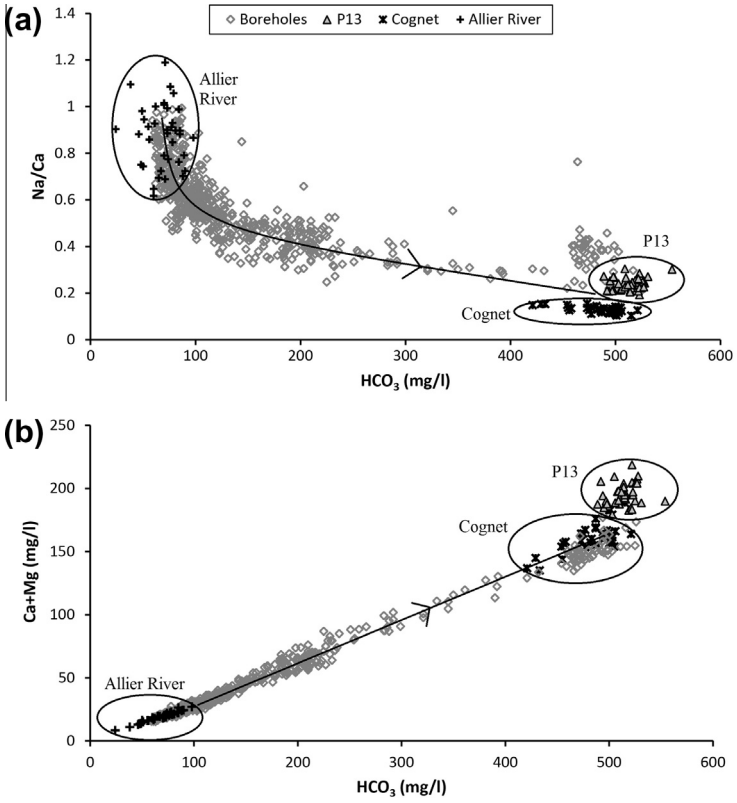

Fig. 11. (a) Na^+/Ca^{2+} vs HCO_3^- and (b) $Ca^{2+} + Mg^{2+}$ vs HCO_3^- plot.

the same variations compared to the Allier River indicating to rapid recharge by water from Allier River, since these points located very close to the Allier River. Whereas, B29 and P13 are oversaturated with carbonate minerals and present a trend similar to Cognet spring demonstrating that these points are recharged partly or mostly by water from hills rather than Allier. This implies, as previously suggested by isotopes, a mixing of the alluvial groundwater with groundwater coming from the hills or from the southern part of the alluvial aquifer.

4.5. Mixing between different sources of recharge

Chloride, nitrate and sulphate ions cannot be related to the dissolution of minerals from the bedrock. Moreover, for these 3 elements, the calculated groundwater concentrations due to rainfall (Cl^- = 4.8 mg/l, NO_3^- = 3.5 mg/l, SO_4^{2-} = 1.1 mg/l) are largely lower than the measured concentrations. These 3 elements could then be attributed to an anthropogenic origin: fertilizers can be implied for [Cl^-], [NO_3^-] and [SO_4^{2-}] in association with [K^+] (Widory et al.,

Table 2
Average values with standard deviation of saturation indices (SI) for carbonate and siliceous minerals.

Sample ID	SI calcite	SI dolomite	SI chalcedony	SI quartz
Allier	−0.9 ± 0.3	−1.9 ± 0.6	−0.2 ± 0.1	0.3 ± 0.1
Cognet	0.5 ± 0.1	0.9 ± 0.3	0.4 ± 0.1	0.8 ± 0.1
P13	0.4 ± 0.1	0.6 ± 0.3	0.3 ± 0.1	0.7 ± 0.1
B10	−0.7 ± 0.2	−1.4 ± 0.3	0.1 ± 0.1	0.5 ± 0.1
B11	−1.2 ± 0.2	−2.6 ± 0.3	−0.1 ± 0.1	0.4 ± 0.1
B18	−1.0 ± 0.1	−2.1 ± 0.2	0.0 ± 0.1	0.4 ± 0.1
B20	−1.1 ± 0.1	−2.4 ± 0.2	−0.0 ± 0.1	0.4 ± 0.1
B23	0.3 ± 0.2	0.6 ± 0.3	0.1 ± 0.1	0.5 ± 0.1
B26	−0.9 ± 0.2	−2.1 ± 0.3	−0.1 ± 0.1	0.3 ± 0.1
B27	−0.4 ± 0.2	−0.8 ± 0.4	0.3 ± 0.1	0.5 ± 0.1
B29	0.4 ± 0.1	0.8 ± 0.2	0.2 ± 0.1	0.6 ± 0.1
B33	−1.3 ± 0.1	−2.6 ± 0.3	−0.1 ± 0.1	0.4 ± 0.1
B39	−0.9 ± 0.2	−1.9 ± 0.4	0.0 ± 0.1	0.4 ± 0.1
B50	−0.6 ± 0.4	−1.3 ± 0.7	−0.0 ± 0.1	0.4 ± 0.1
B56	−0.7 ± 0.2	−1.6 ± 0.5	0.0 ± 0.1	0.5 ± 0.1
B65	−0.4 ± 0.1	−0.9 ± 0.2	0.1 ± 0.1	0.5 ± 0.1
B66	−0.7 ± 0.2	−1.5 ± 0.3	−0.0 ± 0.1	0.4 ± 0.1
B71	−0.6 ± 0.1	−1.4 ± 0.3	0.1 ± 0.1	0.5 ± 0.1

2005), waste waters for NO_3^-, and de-icing salt for [Cl^-] (Meybeck, 1983; Négrel, 1999). In our study area, NO_3^- range from below detection limit (<1) in the boreholes close to Allier River up to 55 mg/l (Table 1) with an average of 15.1 mg/l, and only 5% of the water samples have a concentration of [NO_3^-] higher than the drinking water standard of 50 mg/l (EEA, 2003). These contaminated waters correspond to samples taken from P13 and Cognet spring (not used for drinking purposes). Fig. 13 shows the spatial distribution of [NO_3^-] measured during the two intensive campaigns achieved in December 2010 (low flow) and June 2012 (high flow). No strong difference can be quoted between the two periods emphasizing a continuous supply of nitrate within the field. It is an argument in favour of an origin in connection with residual waters. In the 15 selected boreholes, the highest [NO_3^-] concentrations are recorded in the eastern and southern parts of the site. In alluvial groundwater, mean [Cl^-] varies (Table 1) from 14.5 ± 2.7 mg/l (B11) to 48.7 ± 2.3 mg/l (B29) and demonstrates a general increase toward east. These values are in the range of the concentrations measured for the end-members: mean chloride content is of 15.2 ± 3.8 mg/l in the Allier River, 35.3 ± 5.4 mg/l in Cognet spring; the highest [Cl^-] value 109 mg/l is recorded the 16/07/12 in piezometer P13 (mean value of 68.4 ± 9.2 mg/l). Same observations can be realised for [SO_4^{2-}] generally associated with K^+. Boreholes present concentrations that vary from 6.4 ± 0.8 mg/l (B39) to 76.3 ± 3.7 mg/l (B29) and from 2.9 ± 0.8 mg/l (B26) to 11.5 ± 1.6 mg/l (B29) for [SO_4^{2-}] and [K^+], respectively. The end-members are characterized by concentrations of 8.1 ± 1.4 mg/l [SO_4^{2-}], 3.4 ± 0.8 mg/l [K^+] for Allier River, 36.7 ± 2.3 mg/l [SO_4^{2-}], 17.9 ± 1.6 [K^+] mg/l for Cognet spring, 117.5 ± 12.8 [SO_4^{2-}] mg/l, 10.9 ± 1.2 [K^+] mg/l for P13 (Fig. 14). Therefore, according to the boreholes' concentrations in [Cl^-], [SO_4^{2-}] and [K^+] falling into the range of the ones of the determined end-members and to the independence of these parameters from the lithology, [Cl^-], [SO_4^{2-}] and [K^+] can be used to determine the participation rate of each end-member to the chemistry of boreholes within the alluvial system.

The mathematical resolution of the 3 equations system with 3 unknown values (Jeuken, 2004) leads to the mean participation percentages of each end-member to the chemical composition of the boreholes selected for the following time investigation (Table 3). The mathematical equations can be written as:

$$X_B = F_a X_a + F_h X_h + F_{sa} X_{sa}$$

$$Y_B = F_a Y_a + F_h Y_h + F_{sa} Y_{sa}$$

$$Z_B = F_a Z_a + F_h Z_h + F_{sa} Z_{sa}$$

where X, Y, and Z are the concentrations of [Cl^-], [SO_4^{2-}] and [K^+] respectively for each borehole (B) and end-members: Allier River (a), hills' aquifer (h) and southern aquifer (sa); F is the contribution of each end-member to the borehole's chemistry.

Based on our dataset that includes only the hills' aquifer and the southern aquifer in the right bank of the Allier River, the contribution of end-members has not been calculated for B50. The results of recharge calculations show that eight boreholes are only recharged by the Allier River (Fig. 15). In parallel, Boreholes B27, B56 and B65 are mainly supplied by the Allier River, but present a secondary

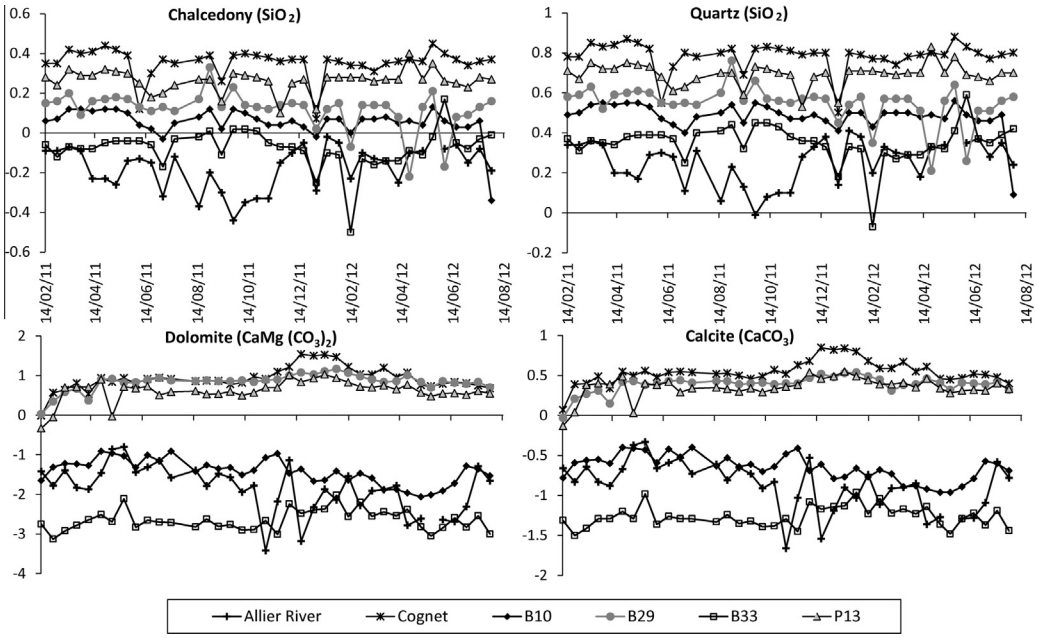

Fig. 12. Plot of saturation indexes (SI) for Allier River, Cognet spring, P13, B33, B10 and B29.

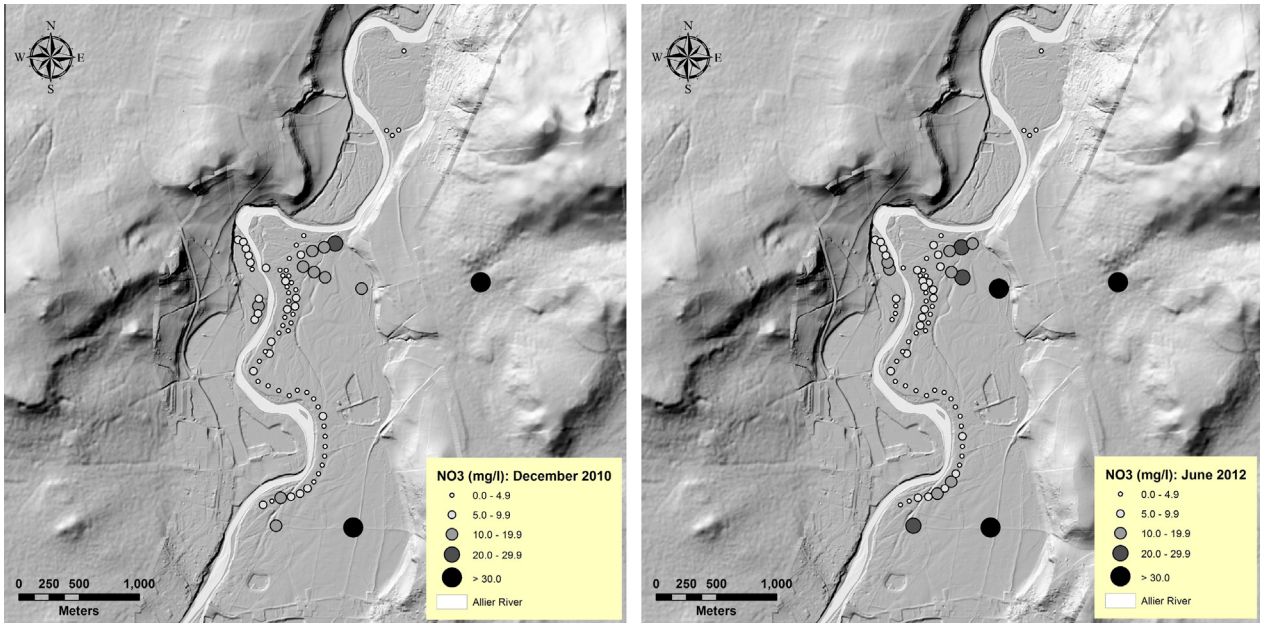

Fig. 13. Spatial distribution of nitrates of 75 points during the two intensive campaigns, (a) December 2010 (low flow period) and (b) June 2012 (high flow period).

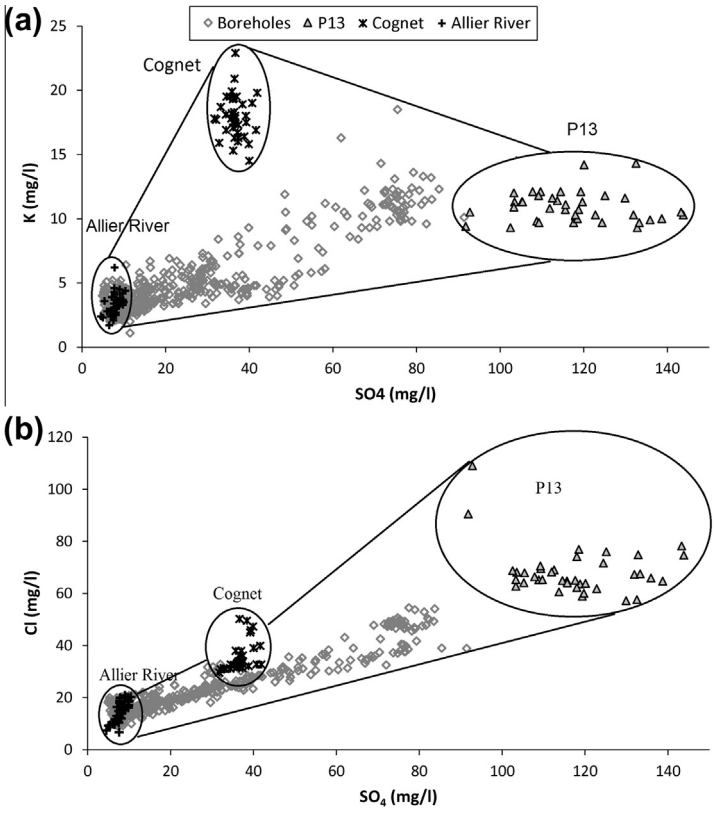

Fig. 14. (a) SO_4^{2-} vs K^+ and (b) SO_4^{2-} vs Cl^- plot.

supply from the southern part of the alluvial aquifer. This latter varies from 11% for B56 to 22% for B27 and is consistent with the location of the boreholes; the lower percentage corresponds to B56 closer to Allier River than B27. High contribution of southern aquifer for B65 (19%) may be due to the sealing of river bank during low flow period; the contribution of Allier River to B56 suggests that the bank is not sealed in this part of the river. Concerning boreholes B23 and B29, results of calculations involve the participation of the three possible origins. As these two boreholes are in the same distance from the hills (Fig. 2), the participation of the volcano-sedimentary aquifer seems to be the same and is evaluated to 27%. The participation of the southern part of aquifer versus Allier River evolved with the increasing distance from the river. Thus B29 presents a higher contribution of the southern part of the alluvial system (56%) whereas B23 displays higher income from the Allier River (37%).

Table 3
Contributions percentage of the 3 end-members.

Borehole ID	Recharge % by Allier River			Recharge % by Hills (Cognet)			Recharge % by South alluvial aquifer (P13)		
	K^+/SO_4^{2-}	K^+/Cl^-	Mean	K^+/SO_4^{2-}	K^+/Cl^-	Mean	K^+/SO_4^{2-}	K^+/Cl^-	mean
B10	87	82	84	0	0	0	13	18	16
B11	100	95	97	0	0	0	0	5	3
B18	100	95	97	0	0	0	0	5	3
B20	100	94	97	0	0	0	0	6	3
B23	33	41	37	23	32	27	44	27	36
B26	100	95	97	0	0	0	0	5	3
B27	79	76	77	0	0	0	21	24	23
B29	17	18	17	27	27	27	56	55	56
B33	100	94	96	0	0	1	0	6	3
B39	100	94	96	0	0	1	0	6	3
B56	90	85	87	2	0	1	8	15	12
B65	81	78	79	3	0	2	16	22	19
B66	98	91	94	0	0	0	2	9	6
B71	98	91	94	0	0	0	2	9	6

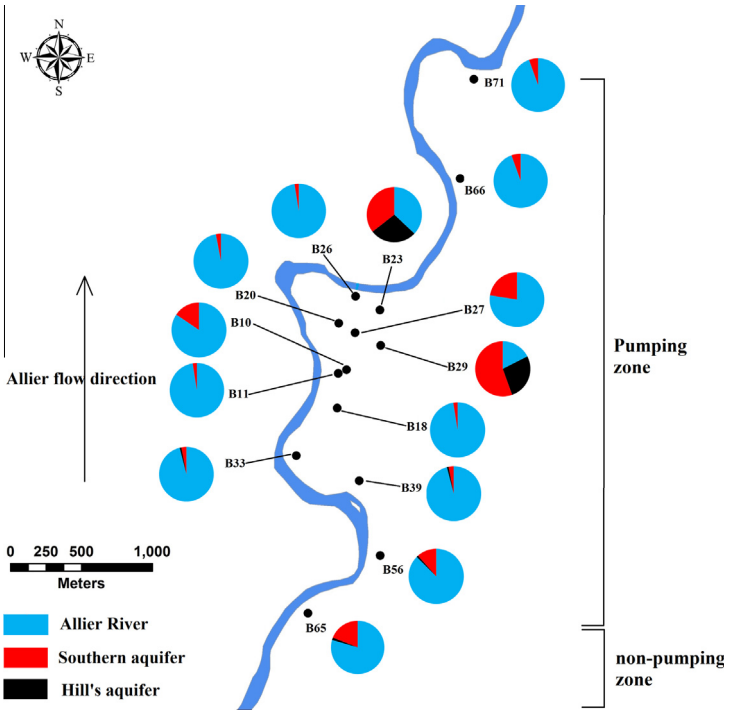

Fig. 15. Calculated percentage contribution of end-members to groundwater samples.

Overall, the contribution of Allier River recharge is significant in the majority of groundwater samples within the alluvial aquifer, contributing up to 100% in boreholes adjacent to it. As expected, the effect of Allier River recharge declines with distance from the river and thus the points far from the river are influenced by either incoming waters from the hills or from the southern part of the alluvial aquifer that modify both their chemical and isotopic signatures.

4.6. Conceptual model of the Allier alluvial aquifer

Groundwater circulates generally from south to north, with a natural alimentation from the hills in the non-pumped part of the alluvial aquifer. 4 end-members have been determined for the recharge of the alluvial groundwater: rainfall, Allier River, surrounding hills' aquifer and the southern part of the alluvial system. Isotopes of the water molecule show that water of the Allier Basin is recharged by rainwater with an evolution from a pole defined by the GMWL and the Allier River, which integrates the influence of the whole watershed to a more local pole defined by the LMWL ($\delta^2H = (7.6 \pm 0.2)\ \delta^{18}O + (1.3 \pm 1.1)$). However, autochthonous recharge by rainfall seems contributing a few to the geochemistry of the alluvial aquifer feeding as only 38% of the total precipitation infiltrate and that effective precipitation harbours major ion concentrations largely below the groundwater contents. Then the chemical content of the investigated boreholes of the alluvial system depends mainly on the contribution of the 3 other end-members. The main recharge is assumed by the Allier River, and then thanks to the water movement generated by the pumping, the water move towards east where the chemistry of boreholes is affected by water/rock interactions and evaporation. On the eastern and southern alluvial aquifer borders, a mixing with waters coming from the hills' aquifer or the southern non-pumped part of the system is shown, notably by the anthropogenic elements such as

nitrates, sulphates (associated with potassium) and chloride. The contribution of the 3 end-members to the boreholes' chemistry has been calculated and shows that Allier River could participate up to 100% in boreholes adjacent to it; this recharge declines with distance from the river (Fig. 15). Boreholes located on the eastern and southern borders are then affected by either incoming waters from the hills or from the southern part of the alluvial aquifer that modify their chemical and isotopic signatures. Locally a probable sealing of the river banks has been highlighted for B65.

5. Conclusions

Considering the fundamental role played by alluvial aquifer in the socio-economic context of a many regions of the world for their uses (drinking, industrial and agricultural purposes) and their ecological role in relation with their connection to surface water, the functioning of these systems has to be well understood. However, due to the interconnection of these systems to many water masses such as precipitation, rivers, pounds, alluvial aquifers, a simple model is not suitable. The complexity of the model increases with the exploitation of this shallow groundwater through large scale pumping what modify the general circulation of groundwater and then their quality. Simultaneous observation and interpretation of spatial and temporal variations in groundwater chemistry and isotope can support the assessment of groundwater recharge sources and contamination by human activities and allow establishing a solid conceptual model that includes water-rock interactions, influence of pumping, recharge and vulnerability. This achievement is fundamental to better understand the system and to elaborate further strategies for alluvial groundwater resource management. Our results supply fundamental results for the groundwater management of the alluvial aquifer of the Allier River. Thus, we highlight that even if rock-water interaction is an important process in the chemical acquisition of groundwater chemistry, anthropogenic activities may threat its quality. Then, contributions of end-members highlight the main issues for protecting groundwater from anthropogenic contamination. Southern and eastern parts of the aquifer suffer from the entrance of groundwater of a lower quality showing the importance of a better definition of the protection's area for drinking water supply. Close to the Allier River, attention should be paid to punctual pollution that may occur in such surface water but also to recurring contamination (due to discharge of waste water treatment plant for example). All this information has to be included in management strategies of groundwater in order to protect sustainability of this valuable resource.

Acknowledgements

The study was financially supported by the European Regional Development Fund (ERDF) through the "Plan Loire Grandeur Nature", the "Agence de l'Eau Loire-Bretagne" (AELB). The authors would like to thank the municipality of Clermont-Ferrand for its financial support and contribution of implementation of the project.

References

Aggarwal P.K., Araguas-Araguas L., Groning M., Kulkarni K.M., Kurttas T., Newman B.D. and Tanweer A. (2009) Laser Spectroscopic Analysis of Liquid Water Samples for Stable hydrogen and oxygen isotopes, IAEA, pp. 49.

Andrade, A.I.A.S.S., Stigter, T.Y., 2011. Hydrogeochemical controls on shallow alluvial groundwater under agricultural land: case study in central portugal. Environ. Earth Sci. 63, 809–825.

Appelo, C.A.J., Postma, D., 1993. Geochemistry, Groundwater and Pollution. Rotterdam, Netherland.

Batard, F., Baubron, J.C., Bosch, B., Marcé, A., Risler, J.J., 1982. Isotopic identification of gases of a deep origin in French thermomineral waters. J. Hydrol. 56, 1–21.

Bertrand, G., Celle-Jeanton, H., Laj, P., Rangognio, J., Chazot, G., 2008. Rainfall chemistry: long range transport versus below cloud scavenging. A two-year study at an inland station (Opme, France). J. Atmos. Chem. 60, 253–271.

Bertrand, G., Celle-Jeanton, H., Huneau, F., Loock, S., Renac, C., 2010. Identification of different groundwater flowpaths within volcanic aquifers using natural tracers for the evaluation of the influence of lava flows morphology. (Argnat basin, Chaîne des Puys, France). J. Hydrol. 391, 223–234.

Bertrand, G., Celle-Jeanton, H., Loock, S., Huneau, F., Lavastre, V., 2013. Contribution of pCO2eq and 13CTDIC evaluation to the identification of CO2 sources in volcanic groundwater systems: influence of hydrometeorological conditions and lava flow morphologies. Application to the Argnat Basin (Chaîne des Puys, Massif Central, France). Aquat. Geochem. 19, 147–171.

Bertrand G. (2009). De la pluie à l'eau souterraine. Apport du traçage naturel (ions majeurs, isotopes) a l'étude du fonctionnement des aquifères volcaniques (Bassin d'Argnat, Auvergne, France). Thèse, Université Blaise Pascal-Clermont-Ferrand II, pp. 96.

Böhlke, J.K., 2002. Groundwater recharge and agricultural contamination. Hydrogeol. J. 10, 153–179.

Bullen, T.D., Krabbenhoft, D.P., Kendall, C., 1996. Kinetic and mineralogic controls on the evolution of groundwater chemistry and 87Sr/86Sr in a sandy silicate aquifer, northern Wisconsin. Geochim. Cosmochim. Acta 60, 1807–1821.

Celle-Jeanton, H., Travi, Y., Loye-Pilot, M.D., Huneau, F., Bertrand, G., 2009. Rainwater chemistry at a Mediterranean inland station (Avignon, France): local contribution versus long range supply. Atmos. Res. 91, 118–126.

Chkirbene, A., Tsujimura, M., CHaref, A, Tanaka, T., 2009. Hydro-geochemical evolution of groundwater in an alluvial aquifer: case of Kurokawa aquifer, Tochigi prefecture, Japan. Desalination 246, 485–495.

Clark, I.D., Fritz, P., 1997. Environmental Isotopes in Hydrogeology. Lewis Publishers, New York.

Craig, H., 1961. Isotopic variations in meteoric water. Science 133, 1702–1703.

Dadet, P., Clozier, L., Giot, D., Fleury, R., Belkessa, R., Batard, F., Carroué, J.P., Jeambrun, M., Châteauneuf, J.J., Farjanel, G., Tourenq, J., 1979. Geological MAP of France at 1:50,000 Scale. BRGM, Orléans.

Dèzes, P., Schmid, S.M., Ziegler, P.A., 2004. Evolution of the European Cenozoic Rift system: interaction of the Alpine and Pyrenean orogens with their foreland lithosphere. Tectonophysics 389, 1–33.

VAN Dorsser H.J., 1969. Etude géomorphologiques dans une partie de la vallee de l'Allier dans la Grande Limagne. Publication ITC, Delft, Pays-Bas, Ser. B50, pp. 66.

Doussan, C., Poitevin, G., Ledoux, E., Detay, M., 1997. River bank filtration: modeling of the changes in water chemistry with emphasis on nitrogen species. J. Contam. Hydrol. 25, 129–156.

EEA (2003). Europe's water: an indicator-based assessment. Topic Report 1/2003, European Environmental Agency, Copenhagen, Denmark, pp. 97. <http://www.eea.europa.eu/publications/topic_report_2003_1>.

European Parliament (2000). Directive 2000/60/EC establishing a framework for Community action in the field of water policy (Water Framework Directive): Official Journal of the European Union. Available via: <http://eur-lex.europa.eu/LexUriServ/LexUriServ.do?uri=CONSLEG:2000L0060:20011216:EN:PDF>.

European Parliament (2006). Directive 2006/118/EC on the protection of groundwater against pollution and deterioration: Official Journal of the European Union. Available at: <http://eur-lex.europa.eu/LexUriServ/LexUriServ.do?uri=OJ:L:2006:372:0019:0019:EN:PDF>.

Fontes, J.C., 1980. Environmental isotopes in ground water hydrology. In: Fritz, P., Fontes, J.C. (Eds.), Handbook of Environmental Isotope Geochemistry. Elsevier, Amsterdam, pp. 75–140.

Frémion M., 1995. Avis sur les mesures de protection du champ captant du Val d'Allier (communes de Cournon, Dallet et Mezel). Département du Puy-de-Dôme.

Frémion, M., 2007. Définition de la nappe d'accompagnement de l'Allier entre Brioude et le Bec d'Allier. Direction régionale de l'environnement, Auvergne.

Friedman, O., Machta, L., Soller, R., 1962. Water vapour exchange between a water droplet and its environment. J. Geophys. Res. 67, 2761–2766.

Gal, F., 2005. Etude géochimique et isotopique des eaux superficielles du bassin versant du Furan et des eaux minérales du graben du forez, est du massif central français, Thèse de 3eme cycle. Université Jean Monnet, Saint-Etienne, 300p.

Gonfiantini, R., 1986. Environmental isotopes in lake studies. In: Fritz, P., Fontes, J.Ch. (Eds.), Handbook of Environmental Isotope Geochemistry, vol. 1. Elsevier, Amsterdam, pp. 113–168.

Guo, H., Wang, Y., 2004. Hydrochemical processes in shallow quaternary aquifers from the northern part of the Datong Basin, China. Appl. Geochem. 19, 19–27.

Hicks, B.B., Shannon, J.D., 1979. A method for modelling the deposition of sulphur by precipitation over regional scales. J. Appl. Meteorol. 18, 1415–1420.

Huggenberger, P., Hoehn, E., Beschta, R., Woessner, W., 1998. Abiotic aspects of channels and floodplains in riparian ecology. Freshw. Biol. 40, 407–425.

Jeuken, B.M., 2004. A Hydrogeochemical Study of the Surficial Aquifers South of Alice Springs, Honours Thesis, Flinders University, Adelaide.

Kelly, W.R., 1997. Heterogeneities in ground-water geochemistry in a sand aquifer beneath an irrigated field. J. Hydrol. 198, 154–176.

Kim, K., 2002. Plagioclase weathering in the groundwater system of a sandy, silicate aquifer. *Hydrol. Process*. 16, 1793–1806.

Klove, B., Allan, A., Bertrand, G., et al., 2011. Groundwater dependent ecosystems. Part II. Ecosystem services and management in Europe under risk of climate change and land use intensification. J. Environ. Sci. 14 (7), 782–793.

Korobova, E.M., Veldkamp, A., Ketner, P., 1997. Element partitioning in sediment, soil and vegetation in an alluvial terrace chronosequence, Limagne rift valley, France: a landscape geochemical study. Catena 31, 91–117.

Kraft, G.J., Sities, W., Mechenich, D.J., 1999. Impacts of irrigated vegetable agriculture on a humid north-central U.S. sand plain aquifer. Ground Water 37, 572–580.

Kroonenberg, S.B., Moura, M.L., Jonker, A.T.J., 1988. Geochemistry of the sands of the Allier river terraces. France. Geologie Mijnb. 67, 75–89.

Livet M., D'Arcy A., Dupuy C., 2006. Synthèse hydrogéologique de l'Auvergne. In '' Aquifères et eaux souterraines en France'', (Ed. BRGM), pp. 956.

Lorite-Herrera, M., Jimenez-Espinosa, R., 2008. Impact of agricultural activity and geologic controls on groundwater quality of the alluvial aquifer of the Guadalquivir River (province of Jaén, Spain): a case study. Environ. Geol. 54, 1391–1402.

Meybeck M. (1983) Atmospheric inputs and river transport of dissolved substances. IAHS Publ. no. 141, 173-192.

Mook W.G., 2000. Environmental isotopes in the hydrological cycle, principles and applications. Volume IV, Groundwater: Saturated and Unsaturated zone.

Nativ, R., Riggio, R., 1989. Meteorologic and isotopic characteristics of precipitation events with implications for ground-water recharge, Southern High Plains. Atmos. Res. 23, 51–82.

Négrel, P., 1999. Geochemical study of a granitic area – The Margeride Mountains, France: chemical element behaviour and 87Sr/86Sr constraints. Aquat. Geochem. 5, 125–165.

Négrel, P., Roy, S., 1998. Chemistry of rainwater in the Massif Central (France): a strontium isotope and major element study. Appl. Geochem. 13, 941–952.

Négrel, P., Petelet-Giraud, E., Barier, J., Guatier, E., 2003. Surface water – groundwater interactions in an alluvial plain: chemical and isotopic systematics. J. Hydrol. 277, 248–267.

Négrel, P., Petelet-Giraud, E., Widory, D., 2004. Strontium isotope geochemistry of alluvial groundwater: a tracer for groundwater resources characterisation. Hydrol. Earth Syst. Sci. 8 (5), 959–972.

Parkhurst D.L., Appelo C.A.J., 2003. User's guide to PHREEQC (Version 2)—A computer program for speciation, batch-reaction, one-dimensional transport, and inverse geochemical calculations: U.S. Geological Survey Water-Resources Investigations Report 99-4259.

Pastre, J.F., 1986. Alteration et palcoalteration des minéraux lourds des alluvions Pliocènes et Pleistocènes du bassin de l'Allier (Massif Central, France). Assoc. Fr. étude Quat. Bull. 3 (4), 257–269.

Pelletier H., 1971. Sur les minéraux lourds transparentes des alluvions anciennes et récentes de la Limagne, d'Auvergne. Thèse III Fac. Sci. Clermont-Ferrand, pp. 76.

Penna, D., Stenni, B., Sanda, M., Wrede, S., Bogaard, T.A., Gobbi, A., Borga, M., Fischer, B.M.C., Bonazza, M., Charova, Z., 2010. On the reproducibility and repeatability of laser absorption spectroscopy measurements for 2H and 18O isotopic analysis. Hydrol. Earth Syst. Sci. 14, 1551–1566.

Rihs, S., Condomines, M., Poidevin, J.-M., 2000. Long-term behaviour of continental hydrothermal systems: U-series study of hydrothermal carbonates from the French Massif Central (Allier Valley). Geochim. Cosmochim. Acta 64, 3189–3199.

Rudel, A., 1963. Les minéraux lourds des terrasses Quaternaires de Limagne d'Auvergne et les éruptions montdoriennes. Soc. Géol. Ft. Bull. 7, 468–469.

Scheytt, T., 1997. Seasonal variations in groundwater chemistry near Lake Belau, Schleswig-Holstein, Northern Germany. Hydrogeol. J. 5, 86–95.

Stallard, R.F., Edmond, J.N., 1983. Geochemistry of the Amazon-II. The influence and the geology and weathering environment on the dissolved load. J. Geophys. Res. 88 (14), 9671–9688.

Stigter, T.Y., van Ooijen, S.P.J., Post, V.E.A., Appelo, C.A.J., Carvalho Dill, A.M.M., 1998. A hydrogeological and hydrochemical explanation of the groundwater composition under irrigated land in a Mediterranean environment, Algarve. Portugal J. Hydrol. 208, 262–279.

Tourenq, J., 1986. Etude sédimentologique des alluvions de la Loire et de l'Allier, des sources au confluent; les mineraux lourds des roches des bassins versants. Documents du BRGM 108, 108.

Veldkamp, A., Feijtel, T.C., 1992. Parent Material Controlled Subsoil Weathering in a Chronosequence, the Allier Terraces, Limagne Rift Valley. France. CATENA 19, 475–489.

Widory, D., Petelet-Giraud, E., Négrel, P., Ladouche, B., 2005. Tracking the sources of nitrate in groundwater using coupled nitrogen and boron isotopes: a synthesis. Environ. Sci. Technol. 39 (2), 539–548.

Wood, W.W., Sanford, W.E., 1995. Chemical and isotopic methods for quantifying ground water recharge in a regional, semiarid environment. Ground Water 33, 458–468.

Ziegler, P.A., Dèzes, P., 2005. Neogene uplift of Variscan Massifs in the Alpine foreland: timing and controlling mechanisms. Variscan Massifs 30 (11), 2005.